Article

Antileishmanial Potential and Chemical Characterization of the Hydroalcoholic Extract Obtained from *Lantana caatingensis* Moldenke (Verbenaceae) Leaves and Its Polar Fractions

Iolanda S. do Carmo,[a] Paulo S. Lima Júnior,[b] Sidney G. de Lima, [a] Jardes F. do Rêgo,[c] Valéria C. de Sousa,[d] Laiz P. Santos,[d] Rita de Cássia V. de Carvalho,[d] Lucas M. M. Marques,[e] Norberto P. Lopes, [e] Fernando Aécio A. Carvalho,[f] José S. Lima Neto *,[g] and Antônia Maria G. L. Citó[a]

[a]*Programa de Pós-Graduação em Química, Universidade Federal do Piauí, 64049-550 Teresina-PI, Brazil*

[b]*Curso de Farmácia, Universidade Federal do Piauí, 64049-550 Teresina-PI, Brazil*

[c]*Departamento de Química, Universidade Estadual do Piauí, 64002-150 Teresina-PI, Brazil*

[d]*Laboratório de Atividade Antileishmania, Núcleo de Pesquisas em Plantas Medicinais, Universidade Federal do Piauí, 64049-550 Teresina-PI, Brazil*

[e]*Núcleo de Pesquisas em Produtos Naturais e Sintéticos, Departamento de Ciências BioMoleculares, Faculdade de Ciências Farmacêuticas de Ribeirão Preto, Universidade de São Paulo, 14040-903 Ribeirão Preto-SP, Brazil*

[f]*Departamento de Biofísica e Fisiologia, Universidade Federal do Piauí, 64049-550 Teresina-PI, Brazil*

[g]*Departamento de Biologia, Centro de Ciências Biológicas e de Saúde, Universidade Federal do Maranhão, 65080-805 São Luís-MA, Brazil*

Lantana caatingensis Moldenke (Verbenaceae) is an endemic plant from northeastern Brazil. However, its chemical composition is almost unknown. This study aimed to characterize the chemical compounds found in *L. caatingensis* and investigate the antileishmanial potential of its hydroalcoholic extract and polar fractions. Compounds present in the hydroalcoholic extract obtained from *L. caatingensis* leaves and its polar fractions (ethyl acetate and methanolic) were analyzed by liquid chromatography with a photodiode-array detector coupled to electrospray ionization quadrupole time-of-flight mass spectrometry. An antileishmanial assay was performed in a 96-well plate against *Leishmania major* promastigotes using resazurin on a plate spectrophotometer and the results were expressed as percentage of growth inhibition. Nine compounds were determined in the investigated extract and fractions, classified as flavonoids, flavonoid *C*-glycosides and phenylethanoid glycosides. The antileishmanial activity revealed that the hydroalcoholic extract and the ethyl acetate fraction were active against *L. major* promastigotes with inhibitory concentration of 71.78 and 26.86 μg mL⁻¹, respectively, while the methanolic fraction was inactive (478.40 μg mL⁻¹). This is the first report on the chemical composition and antileishmanial activity of *L. caatingensis* extracts. These results contribute to further knowledge of species belonging to the *Lantana* genus.

Keywords: flavonoids, phenylethanoids, mass spectrometry, promastigotes, natural products

Introduction

The *Lantana* Linnaeus genus along with *Lippia* genus, are considered the most representative *Lantaneae* tribe members, concentrated in South America and comprising about 129 species.[1] Plants belonging to this genus exhibit shrubby and herbaceous characteristics and are popularly used in the treatment of rheumatism, fever and respiratory diseases, such as flu and colds.[2] A high diversity of secondary metabolites is observed in this genus, such as flavonoids, glycosides phenylethanoids, steroids and triterpenoids, among others.[3]

*e-mail: jose.sln@ufma.br
Editor handled this article: Hector Henrique F. Koolen (Associate)

Lantana caatingensis Moldenke, Verbenaceae, from tribe *Lantaneae*, is a native and endemic shrub from northeastern Brazil. The literature on its chemical composition and biological potential is scarce, although some reports are available on the composition of its essential oil extracted from leaves, which displays antibacterial and modulating activity.[2] Thus, it becomes required to investigate the chemical composition of the species and evaluate its biological potential.

Studies related to natural products utilizing hyphenated analytical techniques, such as liquid chromatography hyphenated with mass spectrometry (LC-MS), enable the simultaneous identification of multiple molecules. The assessment of plant extracts and fractions contributes to the rapid separation of constituents within the plant matrix, resulting in a more precise selection process. Consequently, this approach enhances the dynamism and cost-effectiveness ratio of chemical analyses in the research of natural products.[4] In this context, this study presents the first report on the chemical LC-MS and antileishmanial activity characterizations of the hydroalcoholic extract (EHALC) obtained from *L. caatingensis* leaves and its ethyl acetate (FAcOEtLC) and methanolic (FMeOHLC) fractions.

Experimental

Lantana caatingensis leaves were obtained in May 2018 in the city of Simões, Piauí (latitude: 07°35'S; longitude: 040°40'W), Brazil. The species was identified by Prof Jorge Yoshio Tamashiro (Universidade Estadual de Campinas) and a voucher specimen was deposited at the Universidade Federal do Piauí, Graziella Barroso Herbarium, under ID 27183 and SisGen registration code A587160.

Extraction and fractionation

Lantana caatingensis leaves were dried at room temperature (25-28 °C) and crushed using a knife mill (Micro SL-30/Solab, Piracicaba, Brazil). The plant material (400 g) was submitted to a 70% (v/v) ethanol (Neon, Suzano, SP, Brazil) maceration extraction for six days, with daily solvent renewals. The solution obtained was concentrated using a rotary evaporator, model 820 (Fisatom, São Paulo, Brazil), at reduced pressure and then freeze-dried in Liotop L101 (LioBras, São Carlos, Brazil). The 55 g resulting hydroalcoholic extract (EHALC) was fractionated employing a silica gel column chromatography (80 × 5 cm, 63-200 µm, Sigma-Aldrich, Saint Louis, USA) and eluted by reducing the pressure using increasing polar solvents: hexane, diclorometane, ethyl acetate and methanol (Neon, Suzano, SP, Brazil) until exhaustion. Four fractions, namely hexane (FHexLC-31.9 mg; 0.06%), dichloromethane (FDCMLC-5.1 g; 9.3%), ethyl acetate (FAcOEtLC-16.8 g; 30.5%) and methanolic (FMeOHLC-21.9 g; 39.8%) were obtained. EHALC, FAcOEtLC, and FMeOHLC were submitted for analysis by LC-MS, and the antileishmanial potential of the extract and its polar fractions was carried out employing *Leishmania major* promastigotes.

Liquid chromatography with photodiode-array detector coupled to electrospray ionization quadrupole time-of-flight mass spectrometry (LC-PDA-ESI-QTOF-MS/MS) analysis

Sample preparation

For LC-MS analyses, the EHALC, FAcOEtLC and FMeOHLC were submitted to the solid phase extraction using C18 cartridges 3 mL 500 mg⁻¹ (Chromabond/Macherey-Nagel®, Düren, Germany) that were pre-activated with 15 mL ultrapure water (Millipore, USA), followed by 15 mL of HPLC-grade methanol (Sigma-Aldrich, Saint Louis, USA) and 15 mL of MeOH/H_2O (9:1, v/v). The samples (10 mg mL⁻¹) were subsequently reconstituted in MeOH/H_2O (9:1, v/v) and filtered through a 0.22 µm polytetrafluoroethylene (PTFE) filter (Phenomenex, Torrance, USA).

Analysis conditions

The samples were analyzed using a liquid chromatograph (Shimadzu, Tokyo, Japan) coupled to micrOTOF-Q II mass spectrometer (BrukerDaltonics, Boston, MA, USA), equipped with an electrospray (ESI) source and a quadrupole time-of-flight analyzer (QTOF, Bruker Daltonics Inc., Billerica, MA, USA). A gradient elution was performed in a binary solvent system consisting of 0.1% formic acid (Sigma-Aldrich, St. Louis, USA) in ultrapure water formic acid (solvent A) and 0.1% formic acid in methanol (solvent B). The gradient for chromatographic separation used was: 0 min, 25% B; 0-60 min, 25-80% B; 60-65 min, 80-100% B and 65-80 min, 100% B, with a photodiode array (PDA) cut at 60 min. An injection volume of 20 µL was employed at a concentration of 1 mg mL⁻¹ and detected at 277 nm. Chromatographic separations were performed using a Luna C18 column (250 mm × 4.6 mm, 5 µm) (Phenomenex®, Torrance, CA, USA), maintained at 40 °C, the mobile phase used was a gradient of methanol and water, ranging from 25 to 80%, as previously described. Mass spectra were acquired in both negative and positive modes within the range of *m/z* 50 to 1500. The mass spectrometer operating conditions were set as follows: 5 Bar nebulizer gas pressure, a drying gas flow rate of 10.5 L min⁻¹, capillary voltage set to 3200 V, ion source temperature at 220 °C, and automatic acquisition

2 of 9

J. Braz. Chem. Soc. **2025**, *36*, 2, e-20240113

of 2 spectra s^{-1}. Automated molecule fragmentation was initiated, targeting the four most intense ions from each spectrum. A collision-induced dissociation energy gradient was applied, ranging from 20 to 105 eV according to the precursor ion. After the MS/MS acquisition, the precursor ion was released. Subsequently, all acquired data were processed utilizing the Bruker Compass DataAnalysis 4.3 software (Bruker Daltonics, Boston, MA, USA).

Antileishmanial activity assay against *Leishmania major* promastigotes

The antileishmanial assay was carried out employing *Leishmania major* promastigotes in the log growth phase. The parasites (1×10^6 leishmania *per* 100 μL medium) were seeded in 96-well plates containing supplemented Schneider's medium. The antileishmanial evaluation was conducted in diluted fractions (800-6.25 μg mL^{-1}) added to the wells, in triplicate. The plate was incubated for 42 h (26 °C) in a biochemical oxygen demand incubator. After the first incubation period, 20 μL of resazurin 1×10^{-3} mol L^{-1} (Sigma-Aldrich, St. Louis, USA) were added to each well and the plate was reincubated until 48 h. Antileishmanial activity was determined using a plate spectrophotometer model ELx800 (Biotek, Vermont, USA), at a maximum wavelength (λ_{max}) of 550 nm. Results were expressed as growth inhibition (in percentage). Amphotericin B (Anf B, 2 μg mL^{-1}) (Cristália, Itapira, Brazil) was used as a positive control and Schneider's medium containing 1×10^6 promastigotes *per* well as a negative parameter, corresponding to 100% parasite viability. Blanks for each concentration were also analyzed and subtracted from the controls.[5,6]

Results and Discussion

LC-MS analysis

The detected constituents in EHALC, FAcOEtLC and FMeOHLC (as depicted in Figures 1 and 2 and detailed in Table 1) encompassed *C*-glycoside flavonoids, flavonoids and phenylethanoid glycosides. The fractionation process yielded a distinct separation of compounds, notably observed in the *L. caatingensis* leaf EHALC extract. The FAcOEtLC fraction had less polar compounds predominantly non-polar compounds (eluted with higher MeOH proportions) along with traces of *C*-glycoside flavonoids. In contrast, the FMeOHLC fraction primarily consisted of phenylethanoid glycosides and *C*-glycoside flavonoids, with the latter being in significant abundance.

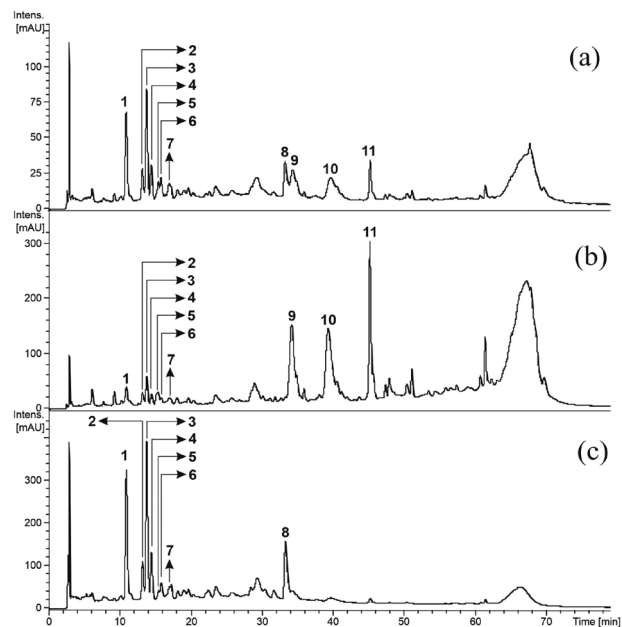For the identification of compounds present in EHALC

Figure 1. LC-PDA chromatograms at 277 nm of the extract and fractions of *L. caatingensis* leaves. Luna C18 column (250 mm × 4.6 mm, 5 μm). (a) Chromatogram of extract (EHALC); (b) chromatogram of fraction FAcOEtLC; (c) chromatogram of fraction FMeOHLC.
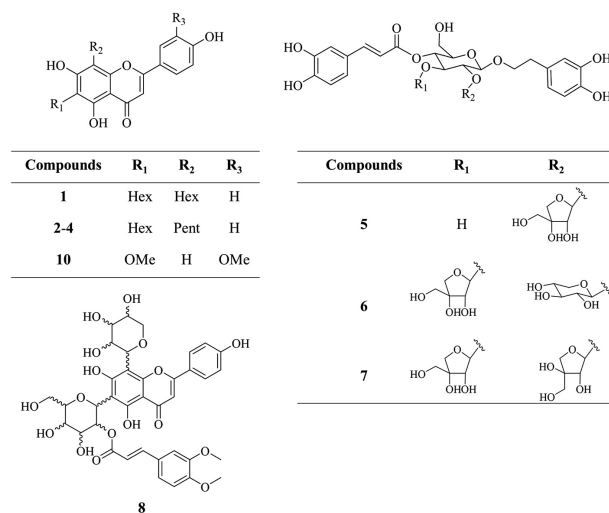

Figure 2. Structure of compounds identified in extract and fractions of *L. caatingensis* leaves. Hex: hexose; Pent: pentose.

and its polar fractions, the wavelength of 277 nm was selected because the chromatogram showed more intense and resolved peaks when compared to other wavelengths.

Peaks **1-4** exhibited absorptions in the UV-Vis spectrum at approximately 270 and 334 nm (Table 1), associated with electronic transitions involving the benzoyl system of the A ring (band II) and the cinnamoyl system of the B ring (band I) of apigenin, respectively.[7] Concerning the MS/MS spectrum of compound **1**, with fragmentation patterns for all compounds outlined in Table 1, a deprotonated molecule, [M − H]$^-$ = *m/z* 593.1527 corresponding to the molecular formula $C_{27}H_{29}O_{15}$ was

Table 1. Compounds detected in extract and fractions of *Lantana caatingensis* by LC-MS

Peak	Retention time / min	Compound	LC-PDA λ / nm	[M − H]− (Δ) / ppm	[M + H]+/ [M + Na]+	Fragments in the negative mode (−)	Fragments in the positive mode (+)	EHALC	FAcOEtLC	FMeOHLC	Reference
1	11.0	apigenin-6,8-C-di-hexoside	216, 270, 334	593.1527 (2.55)	595/−	473 [M − H − 120]−, 383, 353	577 [M + H − 18]+, 559, 541, 475, 457 [M + H − 18 − 120]+, 439, 355, 325, 295	✓	✓	✓	8-10
2	13.3	apigenina-6-C-hexose-8-C-pentoside	216, 270, 334	563.1400 (−1.12)	565/−	503 [M − H − 60]−, 473, 443, 383; 353; 297	547 [M + H−18]+, 529, 511, 475, 427 [M + H − 18 − 120]+, 409, 355, 337, 121	✓	✓	✓	10-13
3	13.9	apigenin-6-C-hexose-8-C-pentoside	216, 270, 334	563.1396 (−1.83)	565/−	503, 473 [M − H − 90]−, 443, 383, 353 [M − H − 120 − 90]−, 297	547 [M + H − 18]+, 529, 511, 475, 427 [M + H − 18 − 120]+, 409, 355, 325, 121	✓	✓	✓	10-13
4	14.6	apigenin-6-C-hexose-8-C-pentoside	216, 270, 334	563.1398 (−1.47)	565/−	473, 443 [M − H − 120]−, 383, 353 [M − H − 120 − 90]−	**547** [M + H − 18]+, 529, 511, 475, 457, 427, 409, 355, 325	✓	✓	✓	10-13
5	15.5	fucatoside A	220, 331	609.1828 (0.51)	−/633	447 [M − H − 162]−	1243 [2M + Na]+, **633** [2M + Na − 610]+, 479, 325	✓	✓	✓	14
6	15.9	fucatoside B	220, 331	741.2247 (−0.07)	−/765	579 [M − H − 162]−, 447 [M − H − 162 − 132]−, 315 [M− H − 162 − 132 − 132]−	457 [M + H − Na − 154 − 132]+, 325	✓	✓	✓	14
7	16.8	fucatoside C	220, 331	741.2240 (−1.01)	−/765	579 [M−H−162]−, 447 [M −H− 162 − 132]−	479 [M + Na − 154 − 132]+, **325**, 163	✓	✓	✓	14
8	33.6	apigenin-6-C-(2″-O-3,4-dimethoxyicinnamoil)-hexose-8-C-pentoside	231, 334	753.1716 (−42.51)	755/−	663[M − H − 90]−, 633 [M − H − 120]−, 545, 425, 353	737 [M + H − 18]+, 719, 635, 617, 529 [M + H − 190 − 18 − 18]+, 511, 475, 427, 409, 391, 337, **325**, 295, 191	✓	−	✓	15,16
9	34.6	U/I	219, 265, 345	315.0551	317/−	**300** [M − H − 15]−	302 [M + H − 15]+, 112 [M + H − 15 − 190]+	✓	✓	−	–
10	40.0	jaceosidin	221, 274, 336	329.0656 (−3.28)	331	**314** [M − H − 15]−, 299 [M −H−15 − 15]−, 271 [M − H − 15 − 15 − 28]−	316 [M + H − 15]+, 273	✓	✓	−	17
11	45.3	U/I	196, 232, 308	305.1772	307/329	**287** [M − H − 18]−	**289** [M + H − 18]+, 271 [M + H − 18 − 18]+, 105	✓	✓	−	–

λ: wavelength observed in nanometers; Δ: mass accuracy; U/I: unidentified; in bold is presented the base peak (100% abundance), in the absence of bold in the fragments, the corresponding base peak becomes the observed molecular ion; ✓: compound present in the analyzed sample. EHALC: hydroalcoholic extract; FAcOEtLC: ethyl acetate fraction; FMeOHLC: methanolic fraction; LC-PDA: UV-Vis absorptions.

observed. Sequential losses of 120 Da ($^{0,2}X_{1,2}^{-}$) were observed in the mass spectrum, indicating the removal of two hexoses units. Fragments *m/z* 353 and 383 indicated the aglycone connected to residual units of 83 and 113 Da, respectively. These fragments suggest the presence of *C*-glycoside apigenin at positions 6 and 8. In the positive mode, the protonated molecule, [M + H]⁺ = *m/z* 595.1291 ($C_{27}H_{31}O_{15}$) gave rise to ions at *m/z* 577, 475 and 457 (base peak). These corresponded to fragments [M + H − 18]⁺, [M + H − 120]⁺ and [M + H − 18 − 120]⁺, respectively. Additionally, ions at *m/z* 355 [M + H − 120 − 120]⁺ and at *m/z* 337 [M + H − 120 − 120 − 18]⁺ confirm the presence of two apigenin *C*-glycosylations. Consequently, peak **1** was assigned as apigenin-6,8-*C*-di-hexoside.[8,9] The mass spectra and proposed fragmentation scheme is shown in Figures S1 and S2 (Supplementary Information (SI) section).

The spectra of **2**-**4** peaks presented a deprotonated molecule, [M − H]⁻ = *m/z* 563 and a protonated molecule [M + H]⁺ = *m/z* 565, assigned as $C_{26}H_{27}O_{14}$ and $C_{26}H_{29}O_{14}$, respectively. Under negative ionization conditions, losses of 60, 90 and 120 Da were observed, attributed to the cleavage of pentose and hexose units, except in the mass spectrum of compound **4**, no loss of 60 Da evident. Ions at *m/z* 383 and at *m/z* 353 were linked to the aglycone apigenin bound with sugar residues, indicative of *C*-glycosylation. In the positive mode of compounds **2** and **3**, sequential 18 Da losses were noted, attributed to water molecules within sugar units. Ions at *m/z* 475 and at *m/z* 445 correspond to the $^{0,2}X_2^{+}$ and $^{0,3}X_1^{+}$ divisions of pentose and hexose, respectively, with the base peak *m/z* 427 indicating the $^{0,2}X_1$ cleavage of hexose followed by the loss of a water molecule. In contrast to compounds **2** and **3**, the MS/MS of **4** indicated the base peak at *m/z* 547, attributed to dehydration. The presence of the ion at *m/z* 355, linked to apigenin with an 85 Da attachment, confirms *C*-glycosylations.[10-12] The proposed fragmentation scheme is shown in Figure 3.
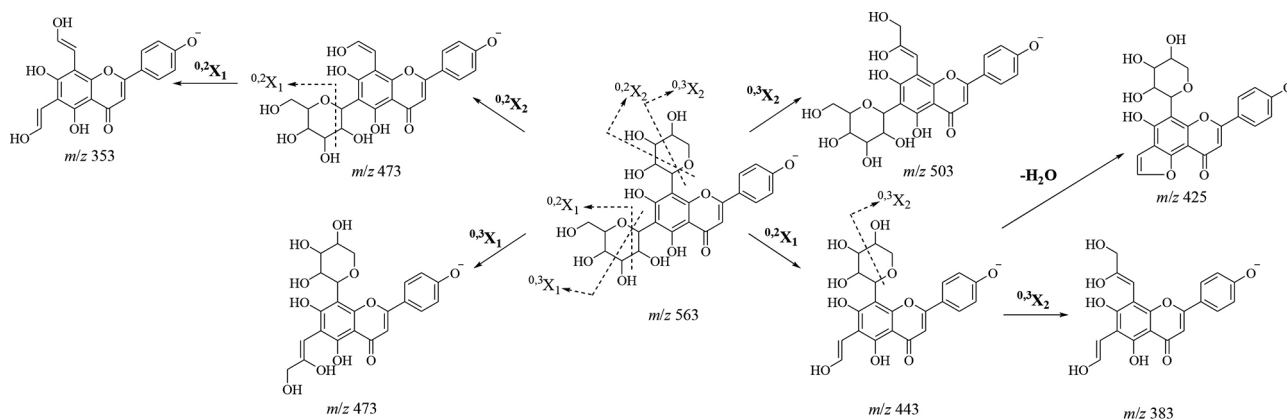
Within flavonoids, *C*-glycosylations are frequently encountered at positions 6 and 8. Identification through mass spectrometry involves observing the relative abundance of ions arising from 60, 90 and 120 Da losses. The fragmentations types $^{0,3}X±$ and $^{0,2}X±$ are attributed to pentoses, along with $^{0,2}X±$ fragmentations for hexoses. However, it's important to note that the loss of 90 Da ($^{0,3}X±$) can also occur in hexoses. Isomers of the 6-*C*-glycoside exhibit significantly higher ion intensities compared to the 8-*C*-glycoside isomer. This phenomenon can be attributed to a stable spatial conformation, alongside the formation of effective hydrogen bonds between the hydroxyl groups at positions 5 and 7 and the carbohydrates. This configuration favors the release of water from sugar units connected at this.[10,13,14]

Based on the data presented in Table 2 and Figure 3, the low abundance of *m/z* 503 (1.5 and 0.9%) in the negative mode of peaks **2** and **3** suggests the presence of pentose at position 8. Conversely, in the positive mode, the relative abundance of ions at *m/z* 427 (100%) and *m/z* 475 (17.7 and 16.1%) signifies hexose at position 6 while and corroborating the presence of pentose at position 8.

Furthermore, an evident preference for 120 Da cleavage, followed by subsequent dehydration, are observed. This corroborates water loss facilitated by hydrogen bonding interactions with hydroxyls at positions 5 and 7, thus supporting the presence of hexose at position 6. It is important to note, the abundance of *m/z* 445 (62%) in the positive ionization mass spectrum of peak **4** strongly suggests that the positioning of hexose at position 6. Conversely, the low abundance of *m/z* 475 (10%), suggests the presence of pentose at position 8. Given the distribution of ions, it is determined that peaks **2**, **3** and **4** are isomers of apigenin-6-*C*-hexose-8-*C*-pentoside isomers (Figures S3 and S4, SI section).[10,13,15]

Regarding the UV-Vis spectrum of compound **8**, significant absorptions were observed approximately at

Figure 3. Scheme of fragmentation of compounds **2**,**3** and **4** in negative mode.

Table 2. Comparison between the relative abundances observed in the MS/MS spectra in the negative and positive mode of **2**, **3** and **4**

Relative abundance of ions in negative mode[a] / %			
Fragment (*m/z*)	**2**	**3**	**4**
563 ([M – H]$^-$)	100	100	100
545 (–H$_2$O)	–	–	–
503 (–^{0,3}X)	1.51	0.94	–
473 (–^{0,2}X and/or – ^{0,3}X)	3.13	3.45	3.39
443 (–^{0,2}X)	2.48	3.45	5.63
425 (–^{0,2}X + H$_2$O)	2.64	2.41	1.13
353 (Agl + 42 + 42 – 1)	26.19	34.15	25.85
383 (Agl + 72 + 42 – 1)	19.84	26.69	18.18
Relative abundance of ions in positive mode[b] / %			
Fragment (*m/z*)	**2**	**3**	**4**
565 ([M + H]$^+$)	12.75	31.42	21.73
547 (–H$_2$O)	34.94	43.27	100
505 (–^{0,3}X)	–	–	–
475 (–^{0,2}X and/or – ^{0,3}X)	17.36	16.10	10.19
445 (–^{0,2}X)	6.58	9.57	62.93
427 (–^{0,2}X + H$_2$O)	100	100	47.60
355 (Agl + 42 + 42 – 1)	7.43	5.84	7.37
385 (Agl + 72 + 42 – 1)	–	–	–

[a]Abundance of ions obtained with energy of 25-50 eV; [b]abundance of ions obtained with energy of 25-62.5 eV. X: hexose or pentose; Agl: aglycone (apigenin).

271 and 334 nm, corresponding to electronic transitions characteristic of apigenin (Figure S5, SI section). The MS/MS analysis of compound **8** revealed a deprotonated molecular, [M – H]$^-$ = *m/z* 753.1716, indicative of the molecular formula C$_{37}$H$_{37}$O$_{17}$. Notably, losses of 90 and 120 Da (*m/z* 663 and 633, respectively) were observed, attributed to the cleavage of pentose and hexose sugar units. Additionally, ions at *m/z* 353 and 383 ions were detected, corresponding to aglycone (apigenin) attached to residual sugar units. These findings provide evidence of apigenin *C*-glycosides at positions 6 and 8.[10] In the positive mode, ions at *m/z* 755.1350 [M + H]$^+$ and *m/z* 777.1124 [M + Na]$^+$ were identified, corresponding to the molecular formulas C$_{37}$H$_{39}$O$_{17}$ and C$_{37}$H$_{38}$O$_{17}$Na, respectively. Within the MS/MS spectrum of the *m/z* 755, sequential losses of 18 Da, indicative of water molecules, were observed. The ions *m/z* 635 [M + H – 120]$^+$ and *m/z* 617 [M + H – 120 – 18]$^+$ originated from the ^{0,2}X$_1$ cleavage of hexose. The determination of sugar positions attached to apigenin was achieved evaluating the relative abundance of ions associated with 90 and 120 Da losses in both spectra.[16] In the negative mode, the ion at *m/z* 633 (9.22%) exhibited a higher abundance compared to that observed for *m/z* 663 (2.47%). Conversely, in the positive mode, the

relative abundance of the ion at *m/z* 635 was 13.72%, with no detection of a 90 Da loss. This information supports the assignment of position 6 to hexose and position 8 to pentose. The abundance of the ion at *m/z* 617 (77.97%) further supports the suggestion of hexose at position 6, as the elimination of water is facilitated by hydrogen bonding interactions with the hydroxyl groups at apigenin positions 5 and 7.[15]

Analyzing the spectra from both ionization modes, it was observed 208 Da loss. However, in the positive mode spectrum 226 Da loss was verified, that corresponds to the 208 Da loss associated to a 18 Da loss, signifying the elimination of a water molecule. The 208 Da mass reduction was attributed to 3,4-dimethoxycinnamoyl, a deduction affirmed by its presence in the formation of the base peak at *m/z* 529. The formation of this ion involves the transfer of a hydrogen atom from the hydroxyl at position 7, followed by dehydration, thus releasing 3,4-dimethoxycinnamoyl in its acid form. The localization of the 3,4-dimethoxycinnamoyl was determined by observing the formation of ions at *m/z* 635 and at *m/z* 617, obtained by the loss of 120 Da. Consequently, it can be inferred that 3,4-dimethoxycinnamoyl is connected to the hexose position 2". Based on this analysis, it was determined that peak **8** corresponds to apigenin-6-*C*-(2"-*O*-3,4-dimethoxycinnamoyl)-hexose-8-*C*-pentoside. Ions at *m/z* 353 and at *m/z* 383 in the negative mode, as well as the ion at *m/z* 355 in the positive mode, alongside the recurring 90 and 120 Da losses, mirror observations made in the **2**-**4** spectra. This similarity points to the likelihood that compound **8** is an acylated derivative of one of these compounds.[16,17] Figure S6 (SI section) represents the fragmentation of compound **8** in the positive and negative ionization modes.

Concerning the UV-Vis spectrum of compound **10**, absorptions were observed at approximately 221, 274 and 336 nm, consistent with the electronic transitions characteristic of flavone flavonoids (Figure S7, SI section). In the negative ionization spectrum, the deprotonated molecule, [M – H]$^-$ = *m/z* 329.0656, aligning with the molecular formula C$_{17}$H$_{13}$O$_7$. Within this spectrum, ions at *m/z* 314 and 299 were observed, indicating sequential methyl losses arising from methoxyls groups (Figure S7). Furthermore, a 28 Da loss was attributed to a CO molecule.[18] In the positive mode spectrum, a methyl and CO loss was observed from the protonated molecule, [M + H]$^+$ = *m/z* 331.0600 (C$_{17}$H$_{15}$O$_7$) (Figure S8, SI section). Based on the observed fragmentations and a comparison with literature data, it can be inferred that peak **10** corresponds to a dimethoxy flavone, it is identified as 3',6-dimethoxy-4',5,7-trihydroxyflavone or jaceosidin.[19]

Peaks **5-7** exhibited absorptions in the UV-Vis spectrum at around 220 and ca. 331 nm corresponding to electronic transitions of the aromatic systems present in the caffeic acid and alcohol 3,4-dihydroxyphenylethanol (Figures S9 and S11, SI section). In the negative ionization mass spectrum of **5**, the precursor ion was $[M − H]^- = m/z$ 609, in agreement with the molecular formula $C_{28}H_{33}O_{15}$. Notably, the MS/MS spectra showed the formation of the ion at m/z 447, indicating a 162 Da loss attributed to a caffeoyl unit. In the positive ionization spectrum, the MS/MS exhibited the ion at m/z 633 $[M + Na]^+$. Additionally, the ion at m/z 1243 $[2M + Na]^+$ was observed and its fragmentation resulted in ions at m/z 633, 479 and 325. This fragmentation pattern was linked to the mass loss associated with 3,4-dihydroxyphenylethanol, reflected in the $[M − 154 + Na]^+$ ion, and the loss of a pentose $[M + H − 154 − 132 − Na]^+$ (Figures S9 and S10, SI section). Based on the information acquired from peak **5**, this compound can be classified as a phenylethanoid glycoside, identified as fucatoside A.[20]

In relation to spectra **6** and **7**, the MS/MS revealed the presence of the ion at m/z 741 ion, corresponding to a deprotonated molecule with the molecular formula $C_{33}H_{41}O_{19}$ (Figure S11). The formation of ions at m/z 579 $[M – H − 162]^-$ can be attributed to the loss of a caffeoyl unit. Additionally, ions at m/z 447 $[M – H – 162 – 132]^-$ and m/z 315 $[M – H – 162 – 132 – 132]^-$ resulting as a consequence of sequential losses of two pentoses. However, it is worth noting that in the spectrum of compound **7**, the ion at m/z 315 was not observed. In the positive ionization spectrum (Figure S11), the compound was identified in the form of adduct with sodium, at m/z 765 $[M + Na]^+$. This led to the formation of m/z 479 through a sequential loss of 154 Da (3,4-dihydroxyphenylethanol) and 132 Da (pentose). Additionally, ions at m/z 457 $[M + H – Na – 154 – 132]^+$ and at m/z 325 $[M + H – Na – 154 – 132 – 132]^+$ were observed (Figure S12, SI section). Upon comparing peaks **6** and **7** with peak **5**, it becomes evident that similar fragments were

formed, suggesting their derivation from compound **5**. The distinguishing factor lies in the mass difference of 132 Da between peak **5** and isomers **6** and **7**. This suggest that the latter compounds carry an additional pentose in comparison to **5**. Hence, **6** and **7** were identified as the phenylethanoid glycosides fucatoside B and C, respectively.[20]

The phenylethanoid glycosides fucatoside A, B and C have been isolated from the leaf extract of *Lantana fucata*.[20] On the other hand, the flavone jaceosidin has been identified in species within the *Lantana* genus, including *Lantana montevidensis* and *Lantana balansae*.[21,22] To date, there is no available data regarding the presence of these metabolites in *L. caatingensis*.

Antileishmanial activity

Both the FAcOEtLC and FMeOHLC fractions inhibited *L. major* promastigote growth in the *in vitro* assay, ranging from 66-93.6% for EHALC and 94-100% for FAcOEtLC. The FMeOHLC fraction resulted in low promastigote inhibition, only 63.4% at the highest concentration investigated (800 µg mL^{-1}). The FAcOEtLC fraction inhibited over 80% of the promastigotes at 50 µg mL^{-1}. No significant inhibitions were observed at 6.25 µg mL^{-1} in relation to the control (Figure 4).

The average 50% inhibitory concentrations (IC$_{50}$) (Table 3) for the samples were determined by a probit regression and compounds were classified as active when IC$_{50}$ ≤ 100 µg mL^{-1}, moderate when IC$_{50}$ ranged between 101 and 199 µg mL^{-1} and inactive when IC$_{50}$ > 200 µg mL^{-1}.[23] The EHALC and the FAcOEtLC fractions presented the lowest IC$_{50}$ values, of 71.78 ± 0.05, 26.86 ± 0.06 µg mL^{-1}, respectively, with FAcOEtLC being the most active, while the FMeOHLC IC$_{50}$ was 478.40 ± 0.03 µg mL^{-1} and, classified as inactive against *L. major* promastigotes. In the protozoan cycle, the promastigote (flagellate form) is the initial infective and circulating form in insect vector and vertebrate hosts, which, after being inoculated, are
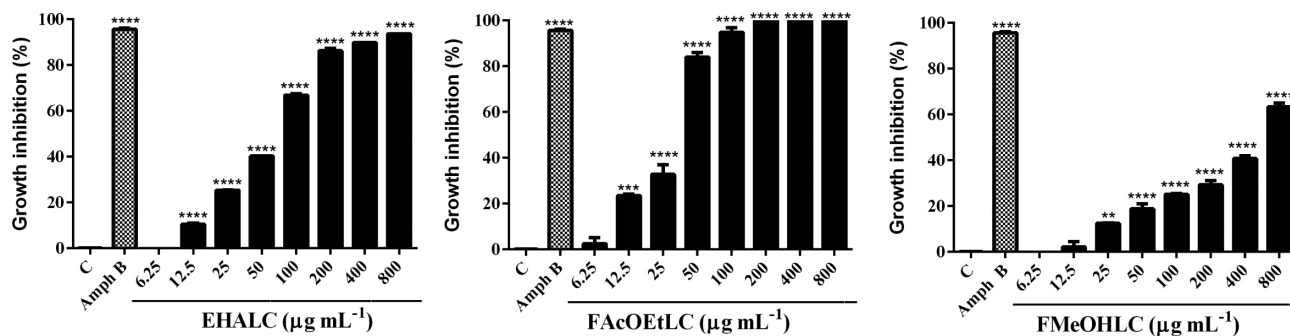

Figure 4. Effect of EHALC, FAcOEtLC, FMeOHLC on growth inhibition of *Leishmania major* promastigotes. EHALC: hydroalcoholic extract; FAcOEtLC: ethyl acetate fraction; FMeOHLC: methanolic fraction; Amph B: amphotericin B (2.5 mg mL^{-1}); control C (Schneider's medium containing 1×10^6 promastigotes). **Significance difference compared to the control, $p < 0.001$ and ****Significance difference compared to the control, $p < 0.0001$.

phagocytosed by macrophages and evolve to the amastigote form (non-flagellated).[24] The IC_{50} findings for the extract and FAcOEtLC fraction may indicate these compounds as candidates for leishmaniasis control by effectively reducing parasite viability.

Table 3. Inhibitory concentrations at 50% (IC_{50}) of the *L. caatingensis* leaf extract and its fractions, calculated by a probit regression

Sample	$IC_{50} \pm SD$ / ($\mu g\ mL^{-1}$)	95% confidence interval / ($\mu g\ mL^{-1}$)	Antipromastigote activity[a]
EHALC	71.78 ± 0.05	50.53-85.39	active
FAcOEtLC	26.86 ± 0.06	21.78-33.08	active
FMeOHLC	478.40 ± 0.03	311.74-894.43	inactive

[a]Antipromastigote activity for the investigated samples was classified considering $IC_{50} \leq 100\ \mu g\ mL^{-1}$ as active, IC_{50} between 101-199 mg mL^{-1} as moderately active and $IC_{50} > 200\ \mu g\ mL^{-1}$ as inactive. EHALC: hydroalcoholic extract; FAcOEtLC: ethyl acetate fraction; FMeOHLC: methanolic fraction; IC_{50}: concentration of compound that provides 50% reduction in parasites; SD: standard deviation.

Antileishmanial activity in extracts from species belonging to the *Lantana* genus have been previously reported, such as the extract and the hexane and ethyl acetate fractions of the aerial parts of *L. balansae*, which are active against *Leishmania braziliensis* promastigotes (IC_{50} = 4.9; 1.3 and 5.3 $\mu g\ mL^{-1}$, respectively) and *L. amazonenses* (IC_{50} = 6; 6.1 and 9.9 $\mu g\ mL^{-1}$, respectively).[21] Antipromastigote activity of the dichloromethane extract (IC_{50} = 18.86-68.40 $\mu g\ mL^{-1}$) obtained from the aerial parts of *L. camara* against *Leishmania mexicana* has also been noted.[25] Therefore, the data obtained from the assays conducted herein and literature data corroborate the antileishmanial potential of the *Lantana* genus and especially *L. caatingensis* as alternative sources of bioactive compounds aimed at leishmaniasis treatment.

Extracts and fractions containing more lipophilic molecules are more permeable to the plasma membrane when compared to more polar molecules, and when these substances contain alkylated substituents, they become promising antiprotozoal activity candidates.[26] Unlike the FAcOEtLC fraction, FMeOHLC presented an IC_{50} 17.8 times higher than that of FAcOEtLC and according to the chromatogram (Figure 1), it is observed that compounds with a lipophilic character are practically absent (indication that the presence of nonpolar compounds in a reversed-phase chromatographic run). However, it is necessary to expand studies on the effect of fractions due to the possible contribution of other associated substances, as well as specifying the major compounds and their action on the promastigote forms of *Leishmania*, in addition to investigating the mechanism of action.

Conclusions

Based on the data analyzed, it was possible to find out the presence of *C*-glycosylated flavonoid, *O*-methoxylated derivatives, and one acylated derivative of apigenin as well as glycosylated phenylethanoids. The activity against *Leishmania major* promastigotes showed, among the samples tested, only the methanolic fraction was inactive ($IC_{50} > 200\ \mu g\ mL^{-1}$), and significant antipromastigote activity of EHALC and FAcOEtLC was observed by other species of the genus *Lantana*. The antileishmanial potential of *L. caatingensis* was demonstrated, however, it is necessary further investigation of the effects of EHALC, FAcOEtLC and FMeOHLC, the possible mechanisms of action of the major compounds and the synergy among the present compounds on promastigotes of *Leishmania major*.

Supplementary Information

Supplementary information is available free of charge at http://jbcs.sbq.org.br as PDF file.

Acknowledgments

Author Contributions

I. S. C. was responsible for investigation, data curation, formal analysis, writing original draft; P. S. L. J. for investigation; S. G. L. for formal analysis, resources; J. F. R. for formal analysis, methodology, writing review and editing, resources; V. C. S. for investigation; L. P. S. for investigation; R. C. V. C. for investigation, validation, data curation; L. M. M. M. for investigation, formal analysis, writing review and editing; N. P. L. for formal analysis, resources, writing review and editing; F. A. A. C. for investigation, methodology, writing review and editing; J. S. L. N. for methodology, validation, investigation, writing review and editing, supervision; A. M. G. L. C. for conceptualization, supervision, resources, project administration, writing original draft.

References

1. Chaitali, A.; Rao, P.; Vikhe, S.; *Res. J. Pharmacogn. Phytochem.* **2022**, *14*, 128. [Crossref]

2. de Aguiar, U. N.; de Lima, S. G.; Rocha, M. S.; Citó, A. M. G. L.; Sousa, A. J. P.; Silva, R. M.; Silva, I. S. A.; da Costa, J. G. M.; *Ind. Crops Prod.* **2015**, *74*, 165. [Crossref]

3. Sousa, E. O.; Costa, J. G. M.; *Rev. Bras. Farmacogn.* **2012**, *22*, 1155. [Crossref]

4. Sashidhara, K. V.; Rosaiah, J. N.; *Nat. Prod. Commun.* **2007**, *2*, 193. [Crossref]

5. Soares, D. C.; Pereira, C. G.; Meireles, M. Â. A.; Saraiva, E. M.; *Parasitol. Int.* **2007**, *56*, 135. [Crossref]

6. Valadares, D. G.; Duarte, M. C.; Oliveira, J. S.; Chávez-Fumagalli, M. A.; Martins, V. T.; Costa, L. E.; Leite, J. P. V.; Santoro, M. M.; Régis, W. C. B.; Tavares, C. A. P.; Coelho, E. A. F.; *Parasitol. Int.* **2011**, *60*, 357. [Crossref]

7. Harborne, J. B.; Mabry, T. J.; Mabry, H.; *The Flavonoids*; Springer: New York, USA, 1975. [Crossref]

8. Liu, S.; Hu, L.; Jiang, D.; Xi, W.; *Molecules* **2019**, *24*, 1755. [Crossref]

9. Zeng, X.; Su, W.; Zheng, Y.; Liu, H.; Li, P.; Zhang, W.; Liang, Y.; Bai, Y.; Peng, W.; Yao, H.; *Molecules* **2018**, *23*, 895. [Crossref]

10. Ferreres, F.; Silva, B. M.; Andrade, P. B.; Seabra, R. M.; Ferreira, M. A.; *Phytochem. Anal.* **2003**, *14*, 352. [Crossref]

11. Gomes, A. C. C.; Sampaio, L. S.; da Silva, P. A.; Lamas, M. E.; Sakuragui, C. M.; Barreto Jr., C. B.; Simas, N. K.; Kuster, R. M.; *Quim. Nova* **2014**, *37*, 1606. [Crossref]

12. Liu, R.; Meng, C.; Zhang, Z.; Ma, H.; Lv, T.; Xie, S.; Liu, Y.; Wang, C.; *Anal. Biochem.* **2020**, *597*, 113673. [Crossref]

13. Cao, J.; Yin, C.; Qin, Y.; Cheng, Z.; Chen, D.; *J. Mass Spectrom.* **2014**, *49*, 1010. [Crossref]

14. Guo, X.; Yue, Y.; Tang, F.; Wang, J.; Yao, X.; Sun, J.; *Int. J. Mass Spectrom.* **2013**, *333*, 59. [Crossref]

15. Zhou, C.; Luo, Y.; Lei, Z.; Wei, G.; *J. Evidence-Based Complementary Altern. Med.* **2018**, ID 8936307. [Crossref]

16. Wang, Y.; Liang, Z.; Liao, X.; Zhou, C.; Xie, Z.; Zhu, S.; Wei, G.; Huang, Y.; *BMC Chem.* **2019**, *13*, 94. [Crossref]

17. Ferreres, F.; Gil-Izquierdo, A.; Vinholes, J.; Grosso, C.; Valentão, P.; Andrade, P. B.; *Rapid Commun. Mass Spectrom.* **2011**, *25*, 700. [Crossref]

18. Demarque, D. P.; Crotti, A. E. M.; Vessecchi, R.; Lopes, J. L. C.; Lopes, N. P.; *Nat. Prod. Rep.* **2016**, *33*, 432. [Crossref]

19. Boukhris, M. A.; Destandau, É.; El Hakmaoui, A.; El Rhaffari, L.; Elfakir, C.; *C. R. Chim.* **2016**, *19*, 1124. [Crossref]

20. Julião, L. D. S.; Piccinelli, A. L.; Marzocco, S.; Leitão, S. G.; Lotti, C.; Autore, G.; Rastrelli, L.; *J. Nat. Prod.* **2009**, *72*, 1424. [Crossref]

21. Maldonado, E. M.; Salamanca, E.; Giménez, A.; Sterner, O.; *Rev. Bras. Farmacogn.* **2016**, *26*, 180. [Crossref]

22. Nagao, T.; Abe, F.; Kinjo, J.; Okabe, H.; *Biol. Pharm. Bull.* **2022**, *25*, 875. [Crossref]

23. Brígido, H. P. C.; da Silva e Silva, J. V.; Bastos, M. L. C.; Correa-Barbosa, J.; Sarmento, R. M.; Costa, E. V. S.; Marinho, A. M. R.; Coelho-Ferreira, M. R.; Silveira, F. T.; Dolabela, M. F.; *Revista Eletrônica Acervo Saúde* **2020**, e3701. [Crossref]

24. Moradin, N.; Descoteaux, A.; *Front. Cell. Infect. Microbiol.* **2012**, *2*, 121. [Crossref]

25. Delgado-Altamirano, R.; García-Aguilera, M. E.; Delgado-Domínguez, J.; Becker, I.; Rodríguez de San Miguel, E.; Rojas-Molina, A.; Esturau-Escofet, N.; *J. Pharm. Biomed. Anal.* **2021**, *199*, 114060. [Crossref]

26. Dagnino, A. P.; de Barros, F. M. C.; Ccana-Ccapatinta, G. V.; Prophiro, J. S.; Poser, G. L. Von; Romão, P. R. T.; *Phytomedicine* **2015**, *22*, 71. [Crossref]

J. Braz. Chem. Soc. **2025**, *36*, 2, e-20240113

9 of 9